Inhibition and Enhancement of the Spontaneous Emission of Quantum Dots in Micropillar Cavities with Radial-Distributed Bragg Reflectors

Tomasz Jakubczyk,[†,‡,*] Helena Franke,[§] Tomasz Smoleński,[†] Maciej Ściesiek,[†] Wojciech Pacuski,[†,‡] Andrzej Golnik,[†] Rüdiger Schmidt-Grund,[§] Marius Grundmann,[§] Carsten Kruse,[‡,⊥] Detlef Hommel,[‡] and Piotr Kossacki[†]

[†]Institute of Experimental Physics, Faculty of Physics, University of Warsaw, Hoża 69, 00-681 Warsaw, Poland, [‡]Institute of Solid State Physics, University of Bremen, P.O. Box 330440, 28334 Bremen, Germany, and [§]Institut für Experimentelle Physik II, Fakultät für Physik und Geowissenschaften, Universität Leipzig Linnéstraße 5, 04103 Leipzig, Germany [⊥]Present address: Fachbereich Physik, Universität Osnabrück, Barbarastrasse 7, 49076 Osnabrück, Germany.

ABSTRACT We present a micropillar cavity where nondesired radial emission is inhibited. The photonic confinement in such a structure is improved by implementation of an additional concentric radial-distributed Bragg reflector. Such a reflector increases the reflectivity in all directions perpendicular to the micropillar axis from a typical value of 15−31% to above 98%. An inhibition of the spontaneous emission of off-resonant excitonic states of quantum dots embedded in the microcavity is revealed by time-resolved experiments. It proves a decreased density of photonic states related to unwanted radial leakage of photons out of the micropillar. For on-resonance conditions, we find that the dot emission rate is increased, evidencing the Purcell enhancement of spontaneous emission. The proposed design can increase the efficiency of single-photon sources and bring to micropillar cavities the functionalities based on lengthened decay times.

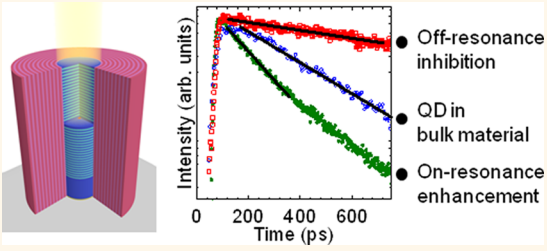

KEYWORDS: micropillar cavity · quantum dot · spontaneous emission inhibition · leaky mode · radial-distributed Bragg reflector · Purcell effect

The need for manipulating light emission and propagation has stimulated the development of photonic structures. The main challenge is to achieve control over the spontaneous emission (SE), specifically to inhibit it when it is not desired and redistribute it into useful forms. In particular it is desired to extract efficiently light emitted from a single quantum dot (QD). Such control is crucial for the application of QDs as sources of single photons[1] and entangled photon pairs.[2] Extraction is an issue for QDs embedded in a bulk semiconductor, because only a few percent of the emitted photons can be collected by the experimental setup. Yet, various techniques of fabrication of the photonic environment allow for increasing the probability of extracting photons from the sample. A few of the best known examples are antireflection coatings,[3] photonic nanowires implementing either conical tapering[4−6] or inverted conical tapering ("trumpet"),[7,8] and back mirrors.[5,6,9] Finally, micropillar cavities[10] not only offer good extraction of photons from the structure but also strongly influence the emission properties of QDs due to the Purcell effect.[11]

In a micropillar cavity light is confined in the vertical direction by upper and lower distributed Bragg reflectors (DBRs). In the horizontal direction it is confined only by the micropillar walls with a high refractive index contrast between the semiconductor and the air. Micropillar cavities are characterized by relatively low mode volumes and high quality factors, which, combined with a method of deterministic preparation of coupled cavity−dot devices,[12] make such cavities one of the best candidates for both applications and fundamental research into light−matter coupling.

In any type of application, the brightness of a coupled micropillar−quantum

* Address correspondence to Tomasz.Jakubczyk@fuw.edu.pl.

Received for review March 31, 2014 and accepted September 2, 2014.

Published online September 02, 2014
10.1021/nn5017555

dot device should be as high as possible. Brightness is defined by the number of collected photons in the first lens of the detection setup per excitation pulse. It is proportional to the emission rate of the dot within the guided mode and inversely proportional to the emission rate into the other, leaky decay channels. The fraction of photons emitted into the mode equals $\beta = F_P/(F_P + G)$, where F_P is the Purcell factor related to the mode and G is the emission rate into other modes. It has recently been proven that a quantum dot in a micropillar device can achieve brightness values as high as 80%[11] due to a highly directional emission profile and the Purcell effect.[13] For standard micropillars, where G equals 1, the 80% is close to the theoretical maximum value of brightness.[11] Further improvement of this value requires a new approach to the design of micropillar structures.

Whereas for standard micropillar structures the reflectivity of DBRs used for vertical confinement can easily reach over 99%,[14] the radial reflectivity equals only about 31% (for typical GaAs-based micropillars) or even less, depending on the semiconductor−air refractive index step. As a consequence, the QD emission is lost through the sidewalls. This transverse emission, commonly described as "leaky" emission, has a great effect on the micropillar's performance. It is a channel through which emitters in micropillars emit photons even if the emission energy is not a resonant energy of the micropillar. As observed for edge emission from planar cavities,[15] this channel is so effective that no inhibition of the emission is observed for detuned emitters.[16−18] Leaky modes also deteriorate the efficiency of single-photon sources, as their presence prevents the emitter from coupling 100% into the desired mode. For these reasons an inhibition of the unwanted emission into leaky modes, which outcouples QD emission in the undesirable planar direction, is one of the major challenges in the micropillar-based cavity technology.

The inhibition of spontaneous emission was first demonstrated for Rydberg atoms[19] in a microwave cavity. For solid-state emitters three-dimensional dielectric periodic structures were proposed,[20] and such structures were used to inhibit the emission of QDs.[21] Strong inhibition was also demonstrated in photonic nanowires[22] and for confined Tamm plasmon modes under metallic microdisks.[23] For micropillar cavities it has been shown that the photonic band gap for the light outcoupling in the transverse directions can be strongly enhanced by means of a silver coating of the micropillars.[24] Suppression of coupling to leaky modes and a large increase in acceleration of the spontaneous emission of QDs resonant with the cavity modes have also been demonstrated for metal-coated micropillars.[25] However, due to losses induced by the metallic coating, this technique is not considered optimal. Furthermore, it does not allow for electrical contacting of micropillars using the existing schemes of contact deposition.[26]

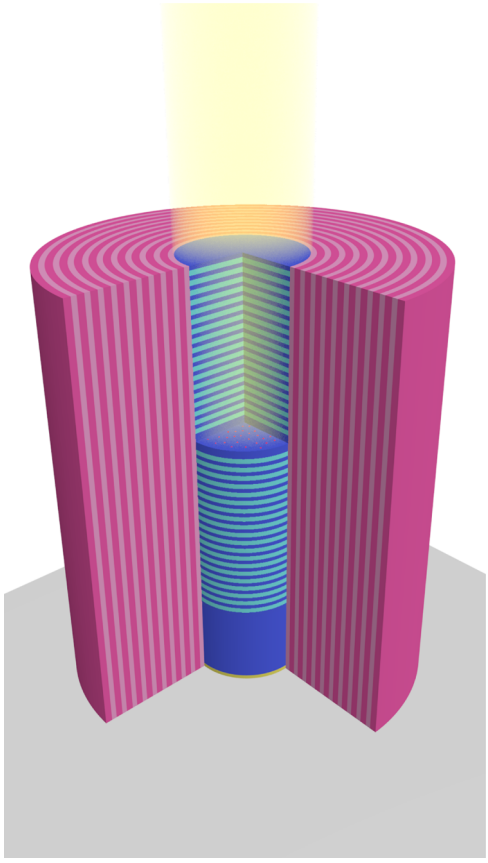

Figure 1. Scheme of a micropillar with a radial DBR. The micropillar is the core of the structure and is coated with cylindrical shell layers constituting a radial-trench DBR.

In the present work, we propose an approach based on coating micropillars with oxide-based radial DBRs[27] assuring over 98% reflectivity[28] in order to effectively suppress emission into leaky modes of the coupled QD−micropillar device[29] (see Figure 1). The presented method is expected to facilitate the construction of future ultrabright light sources approaching the ultimate 100% limit of photon extraction efficiency.

RESULTS AND DISCUSSION

The method of coating with radial DBRs,[27] which can be applied to any semiconductor system, is demonstrated for the recently developed ZnTe-based micropillars containing CdTe/ZnTe QDs.[16,30,31] Both single QD lines and cavity modes were successfully identified in such structures,[32,33] and modes with quality factors of up to 3700 were observed.[34] Recently a Purcell enhancement of emission was demonstrated for a QD at resonance with such a micropillar mode.[16]

We prepared a series of ZnTe-based micropillars (for more details see the Methods section). The distribution of the QDs inside each pillar is purely statistical. However, we have obtained several micropillars with exactly one QD emitting in the spectral range close to the fundamental mode. This allows us to investigate effects resulting from the coupling of a single QD line

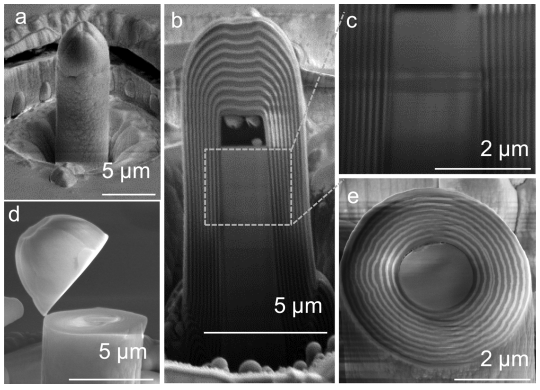

Figure 2. Scanning electron microscope images of micropillars. (a) Micropillar after oblique incidence pulsed laser deposition coating; (b, c) cross-section of a micropillar showing the smooth interface between the micropillar and the radial coating; (d) top of the micropillar during the removal process; (e) top surface of the final micropillar structure showing a cross-section of the radial coating layers.

with a single cavity mode. We also obtained a number of pillars with an increased number of QDs in the range of energies corresponding to micropillar eigenmodes, which enables to investigate spectral characteristics of these modes.[10] Detailed optical characterization of the micropillars is presented in the Supporting Information.

The micropillars were coated with a shell of radial DBRs (see Figure 2) by means of oblique incidence pulsed laser deposition (OIPLD).[27] In order to obtain a homogeneous concentric coating of the micropillars, the plasma plume axis was tilted by about 30° with respect to the normal of the rotated substrate. The DBRs consist of 10 pairs of alternating Al_2O_3 and yttria-stabilized zirconia (YSZ) layers. The ceramic targets were ablated using a pulsed KrF excimer laser at 248 nm with a pulse duration of 25 ns and a fluence of about 2 J/cm^2 at a repetition rate of 15 Hz. Both materials were deposited at a substrate temperature of about 150 °C and an oxygen partial pressure of 0.002 mbar. This relatively low substrate temperature leads to amorphous but smooth DBR layers. The refractive index contrast of the two materials used is about 0.5 (at the investigated wavelengths: n(Al_2O_3) = 1.7 and n(YSZ) = 2.2),[27] leading to a stopband width of the DBR of about 400 meV. With 10 layer pairs the maximum reflectivity amounts to 98.7% at the center of the stopband at 2.2 eV, as deduced from planar samples by means of spectroscopic ellipsometry. This stopband covers the whole range of emission of the ensemble of QDs. During the process a planar DBR grows between the micropillars; however it does not influence the investigated properties of the micropillars.

In order to avoid destructive optical interference in the top layers deposited by OIPLD, the upper part of the coating, a sort of cap on top of the micropillars, has to be removed. Such capping has undesired optical properties, as it deflects luminescence back downward, which was confirmed by low luminescence intensity in experiments on micropillars after OIPLD (not shown). The caps were removed by a focused ion beam (FIB) in a configuration where the beam is perpendicular to the axis of the micropillars (see Figure 2d). This enables precise removal of the cap down to the top layer of the initially uncoated micropillar (see Figure 2e).

A photoresist layer on top of the micropillar, which can be seen in Figure 2b, results from an optional two-step etching procedure of the initial micropillars described in ref 15.

The additional layers deposited on the planar sample mostly peeled off (see Figure 2a, peeling of layer behind the micropillar cavity), while all the coating on the micropillars proved to be stable and durable despite repetitive cooling and possible temperature gradients induced by laser excitation of the micropillars during spectroscopic experiments. The deposited material might introduce compressive or tensile strain on the micropillars[35] depending on the relative thermal expansion coefficients, but no signature of such influence was observed in our experiments.

Longitudinal and cross-sectional cuts of the coated micropillars reveal the high structural quality of the radial DBR. The scanning electron microscope (SEM) pictures of the two surfaces depicted in Figure 2b, c, and e reveal homogeneous layers with smooth interfaces. The designed thicknesses of a DBR layer pair was 157.5 nm, and the value measured with SEM equals 156.2 $\pm$ 7.1 nm. On very few micropillars an inhomogeneity of the radial layer thickness is revealed in horizontal cross-sections, and an example is presented in Figure 2e. Such inhomogeneity may be related to imperfections in the growth of the polycrystalline material or contamination of the sample during the transfer between consecutive technological steps. As discussed later, it may degrade the quality factor of microcavity modes in micropillars featuring such inhomogeneity.

The micropillars were characterized by spectroscopic methods before and after the deposition of radial DBRs. In both cases, at lower temperatures, single QD emission lines were observed. At temperatures of several tens of kelvins, in micropillars with a high number of QDs emitting in the spectral range of the modes, the broadened spectral emission of this ensemble of QDs served as an internal light, revealing eigenmodes due to the photonic confinement[10] (see the Supporting Information).

In order to asses the influence of radial DBR on the optical characteristics of the micropillars, we have determined the quality factor of the fundamental mode for both types of structures. The photoluminescence spectra were collected at a temperature of 70 K and at relatively high optical excitation power. This sets optimal conditions for determination of the quality factor.[34,36] In the case of investigated structures the

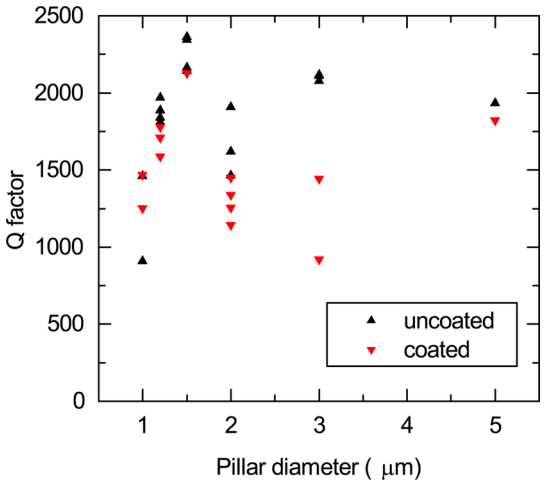

Figure 3. Quality factors of selected micropillars before and after deposition of radial DBR.

spectral density of QD emission was optimized for experiments on investigations of single QD emission lines in the spectral vicinity of modes. Only for selected micropillars was the emission background of QDs uniform enough for determining the optical mode quality factor (spectra are presented in the Supporting Information). Determined quality factors are presented in Figure 3. For micropillars without radial DBR we observe a typical behavior: the quality factor decreases for small diameters due to sidewall scattering.[37] Independent from this trend we observe also an oscillatory behavior of the quality factor. This is also expected for micropillar structures and results mainly from the hybrid character of the cavity mode in the small diameter limit.[38] The guided modes of the microcavity layer couple to modes with different numbers of radial and azimuthal nodes in the DBRs.[38] Such behavior was observed also in other material systems.[39,40] In the case of micropillars investigated in the presented work, for micropillars with a diameter of 1.5 μm the quality factor features a local maximum, which was also observed in previous series of such micropillars.[34]

For micropillars with a diameter of 1.5 μm used in our experiments the achieved value above 2000 is a standard value obtained in this material system.[34] The origin of the low quality factor obtained for larger diameters remains unclear; however minor mistakes during the production process using FIB may cause significant lowering of the quality factor, and the number of micropillars is too low to draw unambiguous conclusions.

For most of the investigated micropillars the quality factor did not significantly change after introduction of radial DBR. Significant changes are observed in the case of micropillars with a diameter of 3 μm. The origin of this difference is unknown and requires further investigations, also including numerical simulations.

An important conclusion is that the radial DBR seems not to be an important source of additional losses for micropillars of small diameter. In our previous investigations[34] we determined that micropillars with diameters of 1.5 μm or smaller are best suited for modifying QD luminescence due to the maximum of the Purcell factor for this diameter.

To prove that the radial DBR inhibits the emission into the continuum of radial leaky modes, we investigated the emission dynamics of the QDs, looking for an increase of the exciton decay time at off-resonance from the cavity modes. Such prolongation, as was mentioned before, is not observed in standard micropillars. For details on the time-resolved experiment see the Methods section.

Our previous studies have shown that the investigated micropillars exhibit a nondegenerate emission of the fundamental mode, which is presumably due to an anisotropy of the refractive index. The fundamental mode energy depends on the orientation of its electric field with a splitting of around 1 meV between the two perpendicular directions, denoted in this paper as polarization X and Y. We used polarization optics in the detection path of the spectroscopic setup to selectively detect photoluminescence related to the investigated mode.

The excitonic emission energy of QDs depends more strongly on the temperature than the energy of the photonic mode and allows spectral tuning of the energy difference,[41] as shown in Figure 4a. We selected a micropillar of 1.5 μm diameter (diameter before the radial coating) with radial DBR, where the QD emission line, labeled QD 1, is at resonance with one of the two states of the fundamental mode of the cavity at a temperature equal to 31 K (X polarization) and with the second one at 19 K (Y polarization).

In the spectral vicinity of the mode there were also other QD emission lines detuned from the micropillar mode in the range from 5 to 80 K (two lines labeled QD 2 and one line labeled QD 3), which served as a reference in the experiment. The attribution of all the emission lines (QD 1, 2, and 3), as related to exciton or charged exciton recombination, was based on an experiment with varying excitation power (not shown). The studied lines 1, 2, and 3, when detuned from the cavity mode, show similar dependence of their intensity *vs* excitation power. Some other emission lines increase faster in intensity when increasing the excitation power, and therefore those other lines can be attributed to higher excitonic complexes (*e.g.*, biexciton). Whether the investigated lines are related to exciton or charged exciton recombination is not relevant in the shown experiments, as both have similar decay dynamics.

Cavity and emitter parameters indicate that the system can be described in the weak coupling regime[17] (indeed there is no Rabi splitting in the photoluminescence spectra). We have investigated the dynamics of the emission lines 1, 2, and 3 by analyzing the temporal profile of their luminescence for various temperatures.

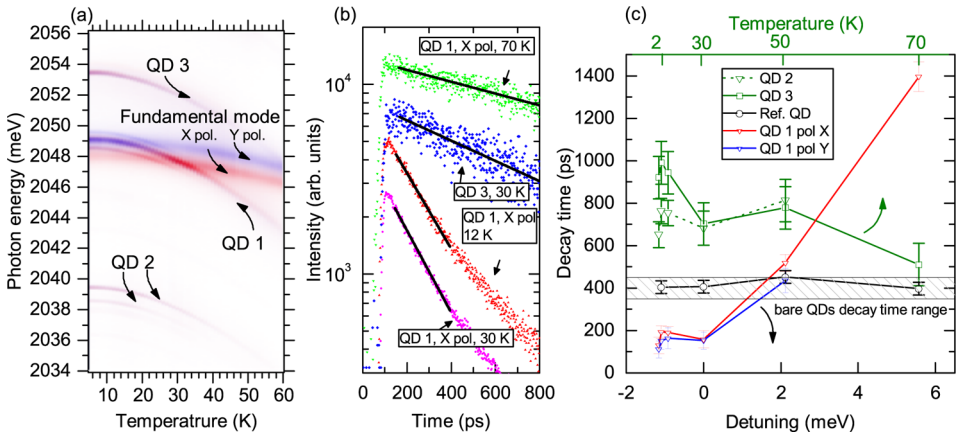

Figure 4. (a) Superposition of two polarization-resolved maps of photoluminescence spectra *vs* temperature (in false color scale) of the 1.5 μm micropillar. Linear polarization is encoded in color, blue (X polarization) and red (Y polarization), and the signal strength is encoded as saturation of the color. (b) Selected decay curves of the QD emission lines collected at various temperatures (detunings) are presented together with exponential fits. The plots are vertically shifted for clarity. (c) Decay times for the QDs in the cavity are shown as a function of detuning. The shaded area marks typical CdTe/ZnTe QD exciton decay time range for QDs without the photonic environment and for QDs in uncoated micropillars out of resonance with cavity modes. The analyzed micropillar has a diameter of 1.5 μm, not including the coating. Additionally the decay time of a reference QD in bulk semiconductor is presented as a function of temperature.

First, we integrated the time-resolved photoluminescence in a 1 meV energy window around the QDs' emission lines. In principle, the decay profiles are expected to be described by more complicated functions than the monoexponential one.[42] This is because the CdTe/ZnTe quantum dots are known to show consequences of the single carrier capture after excitation by a laser with an energy above the energy gap of the barrier material.[43,44] Also tunneling of excitons between dots should lead to slower decay rates.[45] Such slower processes are particularly visible in our experimental data when the fast decay time is short. Our experimental data do not allow determining all details of the complex decay process; however we are convinced that the main fast component at the decay is related to the dipolar radiative recombination of the exciton state formed by the fast initial relaxation, which takes place in tens of picoseconds and is seen as a rise time. Compared to monoexponential, fitting biexponential functions yields times different by only 5% for emitters out of resonance. For resonance condition, however, the change is more important. For instance, in the case of Y-polarized emission it leads to a value of 77 ps (the fast decay component) instead of 147 ps. This range of times gives in our opinion uncertainty of the determination of the radiative decay time in the condition of the resonance. We preferred to remain cautious and have chosen the average value for the later analysis keeping in mind significant experimental uncertainty.

The presence of a dark exciton state might also contribute in the slow decay time, but in CdTe/ZnTe dots it was shown to be negligible at the lower temperature range,[46] for which we see the resonant shortening of the decay time.

The decay times obtained in the described fitting procedure are shown in Figure 4c. The expected lifetime for an exciton (or charged exciton) in CdTe QDs embedded in a standard ZnTe matrix lies in the range between 340 and 450 ps.[16,43] It is clearly visible that the decay of the QD 1 line in resonance with the photonic mode is significantly faster, while the off-resonant emission of all the lines is much longer.

To confirm that the change in the decay time is not related to the temperature variation, we performed a similar experiment on a reference exciton line and used QDs in an unstructured environment (the reference sample; for details see the Methods section). A constant value of the decay time of around 422 ps was obtained. This value is in agreement with results known for CdTe/ZnTe QDs.[43]

One of the terms in the Purcell enhancement factor of spontaneous emission (see ref 17) accounts for the orientation of the emitter dipole with regard to the cavity mode field. In previous reports it was shown that the polarization of the emission of quantum dots embedded within the micropillars can be controlled by coupling it with a polarized photonic mode, such as the fundamental mode of a micropillar with an elliptical cross-section.[47] In such a micropillar also a rotation of the polarization axis and a change of polarization degree are observed as the coupling is varied.[48]

Decay times of QD 1 in both polarizations feature a similar pattern when plotted *vs* temperature. It shows minima for both of the resonances of the QD with the two polarizations of the fundamental cavity mode. This can be explained by assuming that the orientations of the dipole moments related to the specific spin states of the QD1 exciton are tilted 45 deg with respect to the X and Y directions of the modes. Purcell enhancement of the emission is proportional to the square of the cosine function of this angle. In the proposed configuration the exciton is equally enhanced by both of the

polarizations when at resonance with each of the modes.

The QD crosses the higher energy mode at a detuning of around −1 meV (not shown on the map in Figure 4a). The emission line named QD 1 has decay dynamics closely related to the detuning from both of the modes. Departure from the expected shape (sum of two Lorentz functions) of the decay time *vs* detuning[49] relation may result from phonon-mediated emission of the QD−cavity system.[50] On the basis of our previous investigations[16] we assume that the oscillator strength of the QDs is constant over the temperature range considered here. The shortening of the decay time at resonance indicates a Purcell enhancement of the emission.[16] For off-resonance, also in the case of QD 2 and QD 3, a considerable lengthening of the emission time is apparent compared to QDs in an unstructured environment[43] and standard micropillars.[16] We attribute this effect to an efficient suppression of the nonresonant recombination channels (*i.e.*, leaky modes) for the QDs.

The factor of inhibition can be written as $G = \tau_{reference}/\tau_{long}$, where τ_{long} is the long decay time observed far from resonance, and $\tau_{reference}$ is the time measured for a reference exciton in a QD embedded in a bulk semiconductor matrix. For QD 1 the inhibition factor has a value of 0.33. The determined value is the lower bound. In fact, nonradiative decay channels may be blurring the effect by shortening the observed τ_{long}. Possibly, the real impact of the radial-distributed Bragg reflector on the spontaneous emission of QDs might be even more pronounced. The micropillar cavity with QD 1 was selected for the described experiment, as it shows the most pronounced Purcell enhancement and inhibition; therefore QD 1 lies probably close to the micropillar axis, where the fundamental mode has its largest electric field amplitude. Randomly located QDs emitting lines labeled QD 2 and QD 3 are presumably located further from the micropillar axis than QD emitting line QD 1. As a consequence, they are more influenced by the nonradiative processes induced by the proximity of the FIB-damaged surface of the micropillar. The robustness of the effect of spontaneous emission inhibition was confirmed by the lengthened decay time in other micropillars studied in the experiment (not shown here).

Using finite-difference time-domain simulations Ho *et al.*[29] have calculated the amount of sidewall leakage in standard micropillars and micropillars with radial DBR (made of air and AlAs/GaAs). They simulate emission of a spectrally broad, isotropic emitter placed at the center of the microcavity. They varied the reflectivity of the upper and lower micropillar DBR and showed that the sidewall emission intensity drops by a factor from 0.20 to 0.76 after the introduction of radial DBRs. This factor is a good measure of the inhibition expected in our experiment. The factor of inhibition depends on the reflectivity of the DBRs, as they determine the possibility of vertical leakage for off-resonant emission. The factor 0.33 determined in our experiment is in agreement with these theoretical estimations. The simulations show however that it can attain higher values. The fact that we do not observe higher values in our experiment might be related to nonradiative decay channels at the sidewalls of the micropillars.

With the experimentally observed decay times we may determine the Purcell factor characterizing the investigated system. The Purcell factor might be written as[17]

$$F_P = \frac{\tau_{reference}}{\tau_{resonance}} - G \qquad (1)$$

In our experiment the average decay time of the reference QD is $\tau_{reference} = 422 \pm 80$ ps, and the decay time at zero detuning is $\tau_{resonance} = 122 \pm 40$ ps (we take the value obtained for Y polarization which is shorter than the value observed for X polarization). Thus, we obtain a Purcell factor $F = 3.4 \pm 1.3$.

The calculated F_P and G allow determining the β factor, which can be written as

$$\beta = 1 - \frac{\tau_{resonance}}{\tau_{long}} = 0.92 \pm 0.03 \qquad (2)$$

We determine the extraction efficiency of the micropillar, given by the value $\beta Q/Q_0$, where Q_0 is the planar cavity quality factor. From Figure 3 moderate Q_0 values can be deduced, which would result in Q/Q_0 close to unity and therefore in record extraction efficiency. However, as measured for another piece of this microcavity sample the Q_0 value equals around 4000.[34] To avoid overinterpretation, this is the value that we take for further calculations. The origin of the moderate Q_0 value deduced from Figure 3 remains unknown; however possible explanations include local sample degradation, local defects, or poorly calibrated FIB parameters used during etching of micropillars with large diameters.

The calculated extraction efficiency of the micropillar equals 0.49. Certainly, this is not a record value, but this results from the moderate Q/Q_0 parameter of our recently developed ZnTe-based micropillars. Also, we preferred to assume the lower value for Q/Q_0 to avoid overinterpretation of our experimental data. We are convinced that by improving this value, *e.g.*, as is demonstrated in the case of mature technology of the III−V-based micropillars,[11] it is possible to obtain the ultimate brightness discussed in the article.

The radial confinement may introduce additional scattering losses, and as a result, the Q factor of the micropillar may be decreased. However, by using Bloch-wave engineering of the micropillars[51] this undesired effect can be eliminated.

As the SE in the in-plane direction is forbidden, the carriers are redistributed to the states with allowed

recombination channels, *i.e.*, the emission in the vertical direction. This could potentially be very important for applications in light sources, such as vertical-cavity surface-emitting lasers. Demonstration of such a hybrid approach also broadens the range of tools for engineering the photonic band gap, which can be used to tailor the local density of photonic states for all quantum emitters.

The prolongation of the recombination time is promising for increasing the time scale for coherent manipulations of an exciton qubit and lifetime of a dark exciton. The latter was shown to be limited only by in-plane (*i.e.*, radial) radiative recombination.[46] The prolongation of its lifetime is desired in possible applications of this complex as a coherently controlled qubit.[52]

The observation of coherent phenomena requires at least the feasibility of optical control over spins of excitons injected in the QD. Creation of such excitons may be not straightforward in our structures, as they decouple quantum dots from quasi-resonant light pulses. However, in the case of the self-assembled CdTe/ZnTe QDs such control can be experimentally achieved by different methods. For example, it might be achieved by utilizing a spin-conserving excitation transfer between two, spontaneously coupled dots, which was demonstrated in ref 53. In this approach, spin-polarized excitons resonantly created in a high-energy QD are transferred to the second, lower-energy QD, where finally they recombine. Since the typically observed energy difference between such dot pairs is about 200 meV,[53] the excitonic optical transition in a high-energy dot may lie outside the microcavity stopband if the low-energy QD is coupled to the fundamental cavity mode. Another possibility of spin-selective optical exctiation of a QD inside a micropillar is simply related to the excitation of higher-energy excitonic levels of the same QD. Even though their energy is likely to be lying inside the stopband, one can always use sufficiently high excitation power to overcome this difficulty. Since the excitation energy in such an approach is well below the barrier energy gap, even high-power excitation will not cause the creation of excitons outside of the dot.

The insulating radial DBR, in principle, allows for electrical contacting of the micropillars (in opposition to metal-coated micropillars). The wide top surface of such micropillars is well suited for deposition of a ring-shaped top electrode using an existing scheme of micropillar contacting described in ref 26. The procedure and the shape of the electrode have to be adapted for the geometry of our micropillars.

Our idea is to deposit the contact at the top face of the radial DBR and put it in contact with the core micropillar. At the same time the upper aperture of the core micropillar has to be as large as possible to enable propagation of the outgoing beam. However challenging, this tasks seems feasible. Electrical carrier injection into QDs is not possible in metal-coated micropillars.

CONCLUSIONS

In conclusion, we have demonstrated operation of a new type of micropillar structure in which emission into the undesired continuum of radial decay channels has been successfully suppressed, resulting in a decrease of the spontaneous emission rate of QDs by a factor of at least 3. Combined with an enhancement of the spontaneous emission into the guided mode, this shows the potential of micropillars with radial DBRs to achieve a brightness of over 90%. Our study thus sets a new perspective on the construction of a QD-based single-photon source reaching ultimate brightness and providing better control of their spontaneous emission.

METHODS

Micropillar Cavities. The growth of the planar structure, which was the basis for the micropillar cavities, was performed by molecular beam epitaxy. The planar DBR contains ZnTe layers as the high refractive-index material and a short-period superlattice (SL) consisting of MgSe, MgTe, and ZnTe layers as the low-index material.[14] For the resonator structure a 20-pair lower DBR and an 18-pair upper DBR are used, resulting in a high level of photon confinement within the microcavity due to the relatively large refractive index step between the two materials ($n_{SL} = 2.5$[14] and $n_{ZnTe} = 3.0$[54]). *In situ* monitoring of the optical reflectivity during growth enabled good control of the layer thicknesses. In the center of the cavity, at the designed antinode position of the electric field, a single layer of CdTe QDs[55] was placed. It was prepared by the amorphous tellurium desorption method.[56] Micropillars with circular cross-sections of diameters ranging from 0.7 to 5 μm were etched by a focused ion beam out of the planar cavity. Compared to standard micropillar preparation, the surrounding material was etched over a wider range and at a deeper level to provide room for the radial DBR layers deposited on the micropillars in the next step. The maximum emission intensity of the ensemble of QDs was designed to be about 2110 meV, while the cavity thickness (which defines the planar cavity mode energy) was targeted at 2050 meV, corresponding to the low-energy tail of the QDs' ensemble emission. We have fabricated several tens of micropillars.

FIB milling results in a dead area in the milled specimen, which may influence the optical properties of the structured sample. There were several studies examining such a dead layer.[57,58] For the same acceleration voltage as we used to mill the micropillars (30 keV) the experimentally measured thickness of the dead layer in III−V semiconductors is around 25 nm, if the material is oriented parallel to the beam.[58] This surely influences the *Q* factor of the micropillars.

Reference Sample. A reference sample with nominally identical QDs in a ZnTe bulk matrix (without DBRs) was grown. On the reference sample mesas of 1 μm diameter were etched to enable spatial selection of single QDs in the spectral range of interest.

Time-Resolved Spectroscopy. The time-resolved optical measurements were performed using a microphotoluminescence setup at temperatures ranging from 2 to 70 K. We used a

microscope objective to focus the excitation laser beam on a spot with a diameter of less than 2 μm. This enabled spatial selection of single micropillars on the sample. The excitation beam was delivered from a continuous wave frequency-doubled YAG laser (532 nm) or frequency-doubled pulsed titanium-sapphire laser emitting 2 ps pulses at a wavelength of 405 nm with a repetition rate of 76 MHz. Such wavelengths are spectrally outside the DBR's stopband. The emitted light was collected by the same microscope objective. It was then dispersed by a grating spectrometer and analyzed by a CCD camera or a SynchroScan Hamamatsu streak camera for time-resolved signal acquisition with 5 ps resolution.

Conflict of Interest: The authors declare no competing financial interest.

Acknowledgment. The authors gratefully acknowledge M. Florian, F. Jahnke, J. Suffczyński, C. Sturm, and P. Senellart for fruitful discussions. The authors gratefully acknowledge financial support by the DAAD, which supported T.J.'s stay in Bremen, by the National Science Center in Poland (DEC-2013/08/T/ST3/00667, UMO-2013/10/E/ST3/00215, UMO-2011/01/N/ST3/04536, and DEC-2011/02/A/ST3/00131), by the Polish Ministry of Science and Higher Education in years 2012−2016 as research grant "Diamentowy Grant", by the Polish Foundation for Science (program "Mistrz"), by a "Lider" grant from The National Center for Research and Development in Poland, and by the European Union Seventh Framework Programme (FP7/2007-2013) under grant agreement No. 316244. H.F., R.S.G., and M.G. acknowledge funding from the Deutsche Forschungsgemeinschaft (DFG) in the frame of the research unit FOR1616 (project SCHM2710/2-1).

Supporting Information Available: In this material a detailed spectral characterization of the cavity modes is presented. Photoluminescence spectra of micropillars were collected before and after the deposition of radial DBRs. Energies of the photonic modes are determined and plotted *vs* micropillar diameter. This material is available free of charge *via* the Internet at http://pubs.acs.org.

REFERENCES AND NOTES

1. Pelton, M.; Santori, C.; Vuckovic, J.; Zhang, B.; Solomon, G. S.; Plant, J.; Yamamoto, Y. Efficient Source of Single Photons: A Single Quantum Dot in a Micropost Microcavity. *Phys. Rev. Lett.* **2002**, *89*, 233602.
2. Dousse, A.; Suffczynski, J.; Beveratos, A.; Krebs, O.; Lemaître, A.; Sagnes, I.; Bloch, J.; Voisin, P.; Senellart, P. Ultrabright Source of Entangled Photon Pairs. *Nature* **2010**, *466*, 217–220.
3. Takemoto, K.; Takatsu, M.; Hirose, S.; Yokoyama, N.; Sakuma, Y.; Usuki, T.; Miyazawa, T.; Arakawa, Y. An Optical Horn Structure for Single-Photon Source Using Quantum Dots at Telecommunication Wavelengths. *J. Appl. Phys.* **2007**, *101*, 081720.
4. Gregersen, N.; Nielsen, T. R.; Claudon, J.; Gérard, J.-M.; Mørk, J. Controlling the Emission Profile of a Nanowire with a Conical Taper. *Opt. Lett.* **2008**, *33*, 1693–1695.
5. Claudon, J.; Bleuse, J.; Malik, N. S.; Bazin, M.; Jaffrennou, P.; Gregersen, N.; Sauvan, C.; Lalanne, P.; Gerard, J.-M. A Highly Efficient Single-Photon Source Based on a Quantum Dot in a Photonic Nanowire. *Nat. Photonics* **2010**, *4*, 174–177.
6. Reimer, M. E.; Bulgarini, G.; Akopian, N.; Hocevar, M.; Bavinck, M. B.; Verheijen, M. A.; Bakkers, E. P.; Kouwenhoven, L. P.; Zwiller, V. Bright Single-Photon Sources in Bottom-Up Tailored Nanowires. *Nat. Commun.* **2012**, *3*, 737.
7. Gregersen, N.; Nielsen, T. R.; Mørk, J.; Claudon, J.; Gérard, J.-M. Designs for High-Efficiency Electrically Pumped Photonic Nanowire Single-Photon Sources. *Opt. Express* **2010**, *18*, 21204–21218.
8. Munsch, M.; Malik, N. S.; Dupuy, E.; Delga, A.; Bleuse, J.; Gérard, J.-M.; Claudon, J.; Gregersen, N.; Mørk, J. Dielectric GaAs Antenna Ensuring an Efficient Broadband Coupling between an InAs Quantum Dot and a Gaussian Optical Beam. *Phys. Rev. Lett.* **2013**, *110*, 177402.
9. Friedler, I.; Lalanne, P.; Hugonin, J. P.; Claudon, J.; Gérard, J. M.; Beveratos, A.; Robert-Philip, I. Efficient Photonic Mirrors for Semiconductor Nanowires. *Opt. Lett.* **2008**, *33*, 2635–2637.
10. Gérard, J. M.; Barrier, D.; Marzin, J. Y.; Kuszelewicz, R.; Manin, L.; Costard, E.; Thierry-Mieg, V.; Rivera, T. Quantum Boxes as Active Probes for Photonic Microstructures: The Pillar Microcavity Case. *Appl. Phys. Lett.* **1996**, *69*, 449–451.
11. Gazzano, O.; de Vasconcellos, S. M.; Arnold, C.; Nowak, A.; Galopin, E.; Sagnes, I.; Lanco, L.; Lemaître, A.; Senellart, P. Bright Solid-State Sources of Indistinguishable Single Photons. *Nat. Commun.* **2013**, *4*, 1425.
12. Dousse, A.; Lanco, L.; Suffczyński, J.; Semenova, E.; Miard, A.; Lemaître, A.; Sagnes, I.; Roblin, C.; Bloch, J.; Senellart, P. Controlled Light-Matter Coupling for a Single Quantum Dot Embedded in a Pillar Microcavity Using Far-Field Optical Lithography. *Phys. Rev. Lett.* **2008**, *101*, 267404.
13. Purcell, E. M. Spontaneous Emission Probabilities at Radio Frequencies. *Phys. Rev.* **1946**, *69*, 681–681.
14. Pacuski, W.; Kruse, C.; Figge, S.; Hommel, D. High-Reflectivity Broadband Distributed Bragg Reflector Lattice Matched to ZnTe. *Appl. Phys. Lett.* **2009**, *94*, 191108.
15. Ściesiek, M.; Gietka, K.; Golnik, A.; Kossacki, P.; Jakubczyk, T.; Pacuski, W.; Kruse, C.; Hommel, D. Toward Better Light-Confinement in Micropillar Cavities. *Acta Phys. Polym., A* **2011**, *120*, 877–879.
16. Jakubczyk, T.; Pacuski, W.; Smoleński, T.; Golnik, A.; Florian, M.; Jahnke, F.; Kruse, C.; Hommel, D.; Kossacki, P. Pronounced Purcell Enhancement of Spontaneous Emission in CdTe/ZnTe Quantum Dots Embedded in Micropillar Cavities. *Appl. Phys. Lett.* **2012**, *101*, 132105.
17. Gérard, J. M.; Sermage, B.; Gayral, B.; Legrand, B.; Costard, E.; Thierry-Mieg, V. Enhanced Spontaneous Emission by Quantum Boxes in a Monolithic Optical Microcavity. *Phys. Rev. Lett.* **1998**, *81*, 1110–1113.
18. Lohmeyer, H.; Kruse, C.; Sebald, K.; Gutowski, J.; Hommel, D. Enhanced Spontaneous Emission of CdSe Quantum Dots in Monolithic II-VI Pillar Microcavities. *Appl. Phys. Lett.* **2006**, *89*, 091107.
19. Hulet, R. G.; Hilfer, E. S.; Kleppner, D. Inhibited Spontaneous Emission by a Rydberg Atom. *Phys. Rev. Lett.* **1985**, *55*, 2137–2140.
20. Yablonovitch, E. Inhibited Spontaneous Emission in Solid-State Physics and Electronics. *Phys. Rev. Lett.* **1987**, *58*, 2059.
21. Lodahl, P.; Van Driel, A. F.; Nikolaev, I. S.; Irman, A.; Overgaag, K.; Vanmaekelbergh, D.; Vos, W. L. Controlling the Dynamics of Spontaneous Emission from Quantum Dots by Photonic Crystals. *Nature* **2004**, *430*, 654–657.
22. Bleuse, J.; Claudon, J.; Creasey, M.; Malik, N. S.; Gérard, J.-M.; Maksymov, I.; Hugonin, J.-P.; Lalanne, P. Inhibition, Enhancement, and Control of Spontaneous Emission in Photonic Nanowires. *Phys. Rev. Lett.* **2011**, *106*, 103601.
23. Gazzano, O.; de Vasconcellos, S. M.; Gauthron, K.; Symonds, C.; Bloch, J.; Voisin, P.; Bellessa, J.; Lemaître, A.; Senellart, P. Evidence for Confined Tamm Plasmon Modes under Metallic Microdisks and Application to the Control of Spontaneous Optical Emission. *Phys. Rev. Lett.* **2011**, *107*, 247402.
24. Poborchii, V.; Tada, T.; Kanayama, T.; Moroz, A. Silver-Coated Silicon Pillar Photonic Crystals: Enhancement of a Photonic Band Gap. *Appl. Phys. Lett.* **2003**, *82*, 508–510.
25. Bayer, M.; Reinecke, T. L.; Weidner, F.; Larionov, A.; McDonald, A.; Forchel, A. Inhibition and Enhancement of the Spontaneous Emission of Quantum Dots in Structured Microresonators. *Phys. Rev. Lett.* **2001**, *86*, 3168–3171.
26. Böckler, C.; Reitzenstein, S.; Kistner, C.; Debusmann, R.; Löffler, A.; Kida, T.; Höfling, S.; Forchel, A.; Grenouillet, L.; Claudon, J.; *et al.* Electrically Driven High-Q Quantum Dot-Micropillar Cavities. *Appl. Phys. Lett.* **2008**, *92*, 091107.
27. Schmidt-Grund, R.; Hilmer, H.; Hinkel, A.; Sturm, C.; Rheinländer, B.; Gottschalch, V.; Lange, M.; Zúñiga-Pérez, J.; Grundmann, M. Two-Dimensional Confined Photonic Wire Resonators−Strong Light−Matter Coupling. *Phys. Status Solidi B* **2010**, *247*, 1351–1364.

28. Sturm, C.; Hilmer, H.; Schmidt-Grund, R.; Czekalla, C.; Sellmann, J.; Lenzner, J.; Lorenz, M.; Grundmann, M. Strong Exciton-Photon Coupling in ZnO-Based Resonators. *J. Vac. Sci. Technol., B* **2009**, *27*, 1726–1730.
29. Ho, Y.-L.; Cao, T.; Ivanov, P. S.; Cryan, M. J.; Craddock, I. J.; Railton, C. J.; Rarity, J. G. Three-Dimensional FDTD Simulation of Micro-Pillar Microcavity Geometries Suitable for Efficient Single-Photon Sources. *IEEE J. Quantum Electron.* **2007**, *43*, 462–472.
30. Kruse, C.; Pacuski, W.; Jakubczyk, T.; Kobak, J.; Gaj, J. A.; Frank, K.; Schowalter, M.; Rosenauer, A.; Florian, M.; Jahnke, F.; *et al*. Monolithic ZnTe-Based Pillar Microcavities Containing CdTe Quantum Dots. *Nanotechnology* **2011**, *22*, 285204.
31. Pacuski, W.; Jakubczyk, T.; Kruse, C.; Kobak, J.; Kazimierczuk, T.; Goryca, M.; Golnik, A.; Kossacki, P.; Wiater, M.; Wojnar, P.; *et al*. Micropillar Cavity Containing a CdTe Quantum Dot with a Single Manganese Ion. *Cryst. Growth Des.* **2014**, *14*, 988–992.
32. Jakubczyk, T.; Kazimierczuk, T.; Golnik, A.; Bienias, P.; Pacuski, W.; Kruse, C.; Hommel, D.; Klopotowski, L.; Wojtowicz, T.; Gaj, J. A. Optical Study of ZnTe-Based 2D and 0D Photonic Structures Containing CdTe/ZnTe Quantum Dots. *Acta Phys. Polym., A* **2009**, *116*, 888–889.
33. Jakubczyk, T.; Pacuski, W.; Duch, P.; Godlewski, P.; Golnik, A.; Kruse, C.; Hommel, D.; Gaj, J. A. Far Field Emission of Micropillar and Planar Microcavities Lattice-Matched to ZnTe. *Cent. Eur. J. Phys.* **2011**, *9*, 428–431.
34. Jakubczyk, T.; Pacuski, W.; Smolenski, T.; Golnik, A.; Florian, M.; Jahnke, F.; Kruse, C.; Hommel, D.; Kossacki, P. Light-Matter Coupling in ZnTe-Based Micropillar Cavities Containing CdTe Quantum Dots. *J. Appl. Phys.* **2013**, *113*, 136504–136504.
35. Voss, L. F.; Reinhardt, C. E.; Graff, R. T.; Conway, A. M.; Shao, Q.; Nikolic, R. J.; Dar, M. A.; Cheung, C. L. Analysis of Strain in Dielectric Coated Three Dimensional Si Micropillar Arrays. *J. Vac. Sci. Technol. B* **2013**, *31*, 060602.
36. Gayral, B.; Gérard, J. M. Photoluminescence Experiment on Quantum Dots Embedded in a Large Purcell-Factor Microcavity. *Phys. Rev. B* **2008**, *78*, 235306.
37. Rivera, T.; Debray, J.-P.; Gérard, J.; Legrand, B.; Manin-Ferlazzo, L.; Oudar, J. Optical Losses in Plasma-Etched AlGaAs Microresonators Using Reflection Spectroscopy. *Appl. Phys. Lett.* **1999**, *74*, 911–913.
38. Lalanne, P.; Hugonin, J.-P.; Gérard, J. M. Electromagnetic Study of the Quality Factor of Pillar Microcavities in the Small Diameter Limit. *Appl. Phys. Lett.* **2004**, *84*, 4726–4728.
39. Lecamp, G.; Hugonin, J.; Lalanne, P.; Braive, R.; Varoutsis, S.; Laurent, S.; Lemaître, A.; Sagnes, I.; Patriarche, G.; Robert-Philip, I.; *et al*. Submicron-Diameter Semiconductor Pillar Microcavities with Very High Quality Factors. *Appl. Phys. Lett.* **2007**, *90*, 091120–091120.
40. Reitzenstein, S.; Gregersen, N.; Kistner, C.; Strauss, M.; Schneider, C.; Pan, L.; Nielsen, T. R.; Höfling, S.; Mørk, J.; Forchel, A. Oscillatory Variations in the Q Factors of High Quality Micropillar Cavities. *Appl. Phys. Lett.* **2009**, *94*, 061108.
41. Kiraz, A.; Michler, P.; Becher, C.; Gayral, B.; İmamoğlu, A.; Zhang, L.; Hu, E.; Schoenfeld, W. V.; Petroff, P. M. Cavity-Quantum Electrodynamics Using a Single InAs Quantum Dot in a Microdisk Structure. *Appl. Phys. Lett.* **2001**, *78*, 3932–3934.
42. Berstermann, T.; Auer, T.; Kurtze, H.; Schwab, M.; Yakovlev, D.; Bayer, M.; Wiersig, J.; Gies, C.; Jahnke, F.; Reuter, D.; *et al*. Systematic Study of Carrier Correlations in the Electron-Hole Recombination Dynamics of Quantum Dots. *Phys. Rev. B* **2007**, *76*, 165318.
43. Kazimierczuk, T.; Goryca, M.; Koperski, M.; Golnik, A.; Gaj, J. A.; Nawrocki, M.; Wojnar, P.; Kossacki, P. Picosecond Charge Variation of Quantum Dots under Pulsed Excitation. *Phys. Rev. B* **2010**, *81*, 155313.
44. Suffczyński, J.; Kazimierczuk, T.; Goryca, M.; Piechal, B.; Trajnerowicz, A.; Kowalik, K.; Kossacki, P.; Golnik, A.; Korona, K.; Nawrocki, M.; *et al*. Excitation Mechanisms of Individual CdTe/ZnTe Quantum Dots Studied by Photon Correlation Spectroscopy. *Phys. Rev. B* **2006**, *74*, 085319.
45. Korona, K.; Wojnar, P.; Gaj, J.; Karczewski, G.; Kossut, J.; Kuhl, J. Influence of Quantum Dot Density on Excitonic Transport and Recombination in CdZnTe/ZnTe QD Structures. *Solid State Commun.* **2005**, *133*, 369–373.
46. Smoleński, T.; Kazimierczuk, T.; Goryca, M.; Jakubczyk, T.; Wojnar, P.; Golnik, A.; Kossacki, P. In-plane Radiative Recombination Channel of a Dark Exciton in Self-Assembled Quantum Dots. *Phys. Rev. B* **2012**, *86*, 241305.
47. Daraei, A.; Tahraoui, A.; Sanvitto, D.; Timpson, J.; Fry, P.; Hopkinson, M.; Guimaraes, P.; Vinck, H.; Whittaker, D.; Skolnick, M.; *et al*. Control of Polarized Single Quantum Dot Emission of High-Quality-Factor Microcavity Pillars. *Appl. Phys. Lett.* **2006**, *88*, 051113–051113.
48. Lee, Y.-S.; Lin, S.-D. Polarized Emission of Quantum Dots in Microcavity and Anisotropic Purcell Factors. *Opt. Express* **2014**, *22*, 1512–1523.
49. Munsch, M.; Mosset, A.; Auffèves, A.; Seidelin, S.; Poizat, J. P.; Gérard, J.-M.; Lemaître, A.; Sagnes, I.; Senellart, P. Continuous-Wave *versus* Time-Resolved Measurements of Purcell Factors for Quantum Dots in Semiconductor Microcavities. *Phys. Rev. B* **2009**, *80*, 115312.
50. Hohenester, U.; Laucht, A.; Kaniber, M.; Hauke, N.; Neumann, A.; Mohtashami, A.; Seliger, M.; Bichler, M.; Finley, J. J. Phonon-Assisted Transitions From Quantum Dot Excitons to Cavity Photons. *Phys. Rev. B* **2009**, *80*, 201311.
51. Lermer, M.; Gregersen, N.; Dunzer, F.; Reitzenstein, S.; Höfling, S.; Mørk, J.; Worschech, L.; Kamp, M.; Forchel, A. Bloch-Wave Engineering of Quantum Dot Micropillars for Cavity Quantum Electrodynamics Experiments. *Phys. Rev. Lett.* **2012**, *108*, 057402.
52. Poem, E.; Kodriano, Y.; Tradonsky, C.; Lindner, N.; Gerardot, B.; Petroff, P.; Gershoni, D. Accessing the Dark Exciton with Light. *Nat. Phys.* **2010**, *6*, 993–997.
53. Kazimierczuk, T.; Suffczyński, J.; Golnik, A.; Gaj, J. A.; Kossacki, P.; Wojnar, P. Optically Induced Energy and Spin Transfer in Nonresonantly Coupled Pairs of Self-Assembled CdTe/ZnTe Quantum Dots. *Phys. Rev. B* **2009**, *79*, 153301.
54. Marple, D. T. F. Refractive Index of ZnSe, ZnTe, and CdTe. *J. Appl. Phys.* **1964**, *35*, 539–542.
55. Kobak, J.; Smoleński, T.; Goryca, M.; Papaj, M.; Gietka, K.; Bogucki, A.; Koperski, M.; Rousset, J.-G.; Suffczyński, J.; Janik, E. *et al*. Designing Quantum Dots for Solotronics. *Nat. Commun.* **2014**, *5*, 3191.
56. Tinjod, F.; Gilles, B.; Moehl, S.; Kheng, K.; Mariette, H. II-VI Quantum Dot Formation Induced by Surface Energy Change of a Strained Layer. *Appl. Phys. Lett.* **2003**, *82*, 4340–4342.
57. Kato, N.; Kohno, Y.; Saka, H. Side-Wall Damage in a Transmission Electron Microscopy Specimen of Crystalline Si Prepared by Focused Ion Beam Etching. *J. Vac. Sci., Technol. A* **1999**, *17*, 1201–1204.
58. Rubanov, S.; Munroe, P. Damage in III-V Compounds during Focused Ion Beam Milling. *Microsc. Microanal.* **2005**, *11*, 446–455.